5.1 (23084) **THE EFFECTS OF NONHYDROSTATIC DYNAMICS IN HIGH RESOLUTION NUMERICAL FORECASTS**

Zavisa I. Janjic NOAA/NWS/NCEP, Camp Springs, MD 20746

1. Introduction

Considerable experience with the nonhydrostatic models has been accumulated on the scales of convective clouds and storms. However, numerical weather prediction (NWP) deals with motions on a much wider range of temporal and spatial scales. Difficulties that may not be significant, or may go unnoticed on the small scales may become important in NWP applications. For example, an erratic gain or loss of mass would be hard to tolerate in operational NWP applications. Another problem may arise regarding the control of spurious motions generated in upper levels by the nonhydrostatic dynamics and numerics. Forcing the variables in the top layers toward a constant in time basic state in response to this problem appears to be inadequate for NWP. On the other hand, specifying time dependent computational top boundary conditions could further limit the ability of the regional nonhydrostatic model to produce more accurate forecasts than the parent hydrostatic model. Finally, experience concerning the benefits that can be expected in NWP from nonhydrostatic models is insufficient.

Having in mind these considerations, a new approach was proposed (Janjic, 2001; Janjic et al., 2001) as an alternative to extending cloud models to synoptic and larger scales. This approach is based on relaxing the hydrostatic approximation in a hydrostatic model using vertical coordinate based on hydrostatic pressure. In this way the applicability of the model is extended to nonhydrostatic motions.

In order to do so, the system of nonhydrostatic equations is split into two parts: (a) the part that corresponds to the hydrostatic system, except for higher order corrections due to vertical acceleration, and (b) the system of equations that allows computation of the corrections appearing in the first system due to the vertical acceleration. The separation of the nonhydrostatic contributions shows in a transparent way how the hydrostatic approximation affects the model equations. The described procedure does not require any linearization or additional approximation. At the same time, the favorable features of the hydrostatic model formulation are preserved within the range of validity of the hydrostatic approximation.

With this approach the nonhydrostatic dynamics is introduced through an add–on module that can be turned on and off depending on resolution. This allows easy comparison of hydrostatic and nonhydrostatic solutions obtained using otherwise identical model.

_____

Corresponding author address: Zavisa Janjic, Room 207, 5200 Auth Rd., Camp Springs, MD 20746; *e-mail:* zavisa.janjic@ncep.noaa.gov

2. The model

The nonhydrostatic models used in this study share all major conservational and other discretization principles (Janjic, 1977, 1979, 1984, 1997; Janjic and Wiin-Nielsen 1977; Janjic et al., 1995) and the physical package (Chen et al., 1997; Janjic, 1990, 1994, 1996a, 1996b, 2000; Zhao and Carr, 1997) with the NCEP Meso (Eta) model. The only notable exception is that the step-mountains (Bryan, 1969; Mesinger et al. 1988), are not used. Namely, with increasing horizontal resolution, several problems surfaced up that could be associated with the step-mountain representation. Consider, for example, the windstorm that occurred on February 24 1997 on the slopes of the Wasatch Front east of Salt Lake City, Utah (McDonald et al. 1998). At that time, NCEP was running the Nest-in-the-West system with the step-mountain option, 10 km horizontal resolution and 60 levels in the vertical. This system did not predict the windstorm.

Searching for the reasons for the failure, parallel tests were made using the step-mountains and the conventional sigma coordinate. In the tests, the non-hydrostatic model was run with a horizontal resolution of 8 km and with 32 layers in the vertical. In order to improve the accuracy of the pressure gradient force in the sigma mode, a scheme was used that reduces to the technique proposed by Janjic (1977) for the hydrostatic atmosphere (see also, Janjic 1998). Vertical cross sections along the 41 N latitude, and extending from 112.80 W to 111.20 W in the horizontal and from 1000 m to 6500 m in the vertical, are shown in Fig. 1 for the 9 hour, 12 hour and 15 hour forecast times (top to bottom) starting from 00 UTC, February 24 1997. The step-mountain results are shown on the left, and the sigma mode results on the right. Isolines of potential temperature and wind vectors in the vertical plain are displayed. The contour interval for the potential temperature is 2 degrees. As can be seen from the figure, in the sigma mode the model successfully developed strong low-level down-slope winds reaching maximum intensity between 12 UTC and 15 UTC. This agrees with observations that showed the strongest wind at 15 UTC (McDonald et al. 1998). An interesting feature is the rapid decrease of the low level wind with increasing distance from the slope that occurred in the sigma mode run. In contrast to that, there was hardly any indication of the storm in the step-mountain run

In addition to the example shown, several recent studies (Adcroft et al, 1997; Galus, 2000, Gallus and Klemp, 2000, Janjic and DiMego, 2001) indicate that further problems should be expected at higher resolutions. In particular, another problem possibly

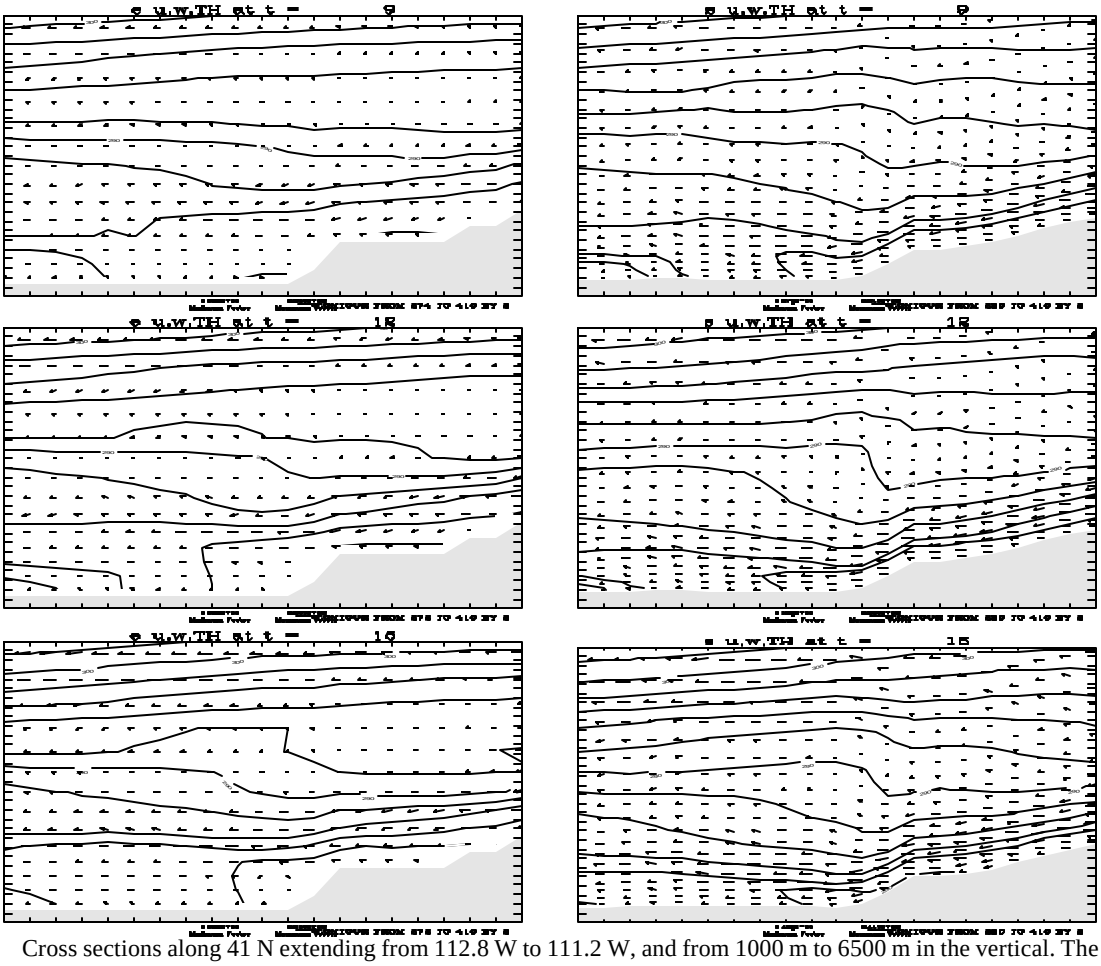

Fig. 1. Cross sections along 41 N extending from 112.8 W to 111.2 W, and from 1000 m to 6500 m in the vertical. The 9 hour, 12 hour and 15 hour forecasts (top to bottom) starting from 00 UTC, February 24, 1997 (eta left, sigma right). The potential temperature and wind vector are shown. The contour interval for the potential temperature is 2 degrees.

related to the mountain representation is that the NCEP Meso model using the step-mountains is producing precipitation too far down on the mountain slopes (Staudenmeier and Mittelstadt, 1998). A similar problem was noticed independently in the operational runs in the Alpine region made at the Regional Weather Service of Emilia-Romagna, Italy (Communicated by Pacagnella). In response to the problem, the Italian meteorologists replaced the step-mountains by the conventional sigma coordinate. In preliminary tests performed at NCEP (e.g., Janjic and DiMego, 2001), a similar signature of the step-mountains was detected.

Thus, the hybrid pressure-sigma vertical coordinate (Arakawa and Lamb, 1977) was chosen as the primary option for the high-resolution nonhydrostatic model. With this choice, the coordinate surfaces are flat above and away from the mountains. In the vicinity of the mountains the hybrid coordinate has increased vertical resolution, and the equations are continuous, without the computational internal boundary conditions that have to be specified with the step-mountains. Note that the hydrostatic pressure is used as the vertical coordinate in the uppermost layers where, generally, largest errors in the sigma coordinate occur. Thus, with the hybrid coordinate, the most serious problems associated with the sloping coordinate surfaces are eliminated. In addition, the increased resolution in the lower layers acts in the direction of reducing the computational inaccuracies, and certainly improves the representation of the PBL over elevated terrain.

3. Nonhydrostatic NWP examples

The differences between hydrostatic and nonhydrostatic forecasts of orographic precipitation at different horizontal resolutions were discussed in Janjic et al (2001). They noticed that the nonhydrostatic dynamics left similar signatures in the runs with both 8 km and 1 km resolutions.

The horizontal resolution chosen for the present study is again 8 km. It is believed that such a relatively coarse resolution is representative for the next generation of continental scale regional models. Within the hybrid vertical coordinate, the sigma coordinate part was employed below 400 hPa. In the first two runs that

will be discussed here, the model had 50 levels in the vertical and the integration domain covered the area of 18 degrees by 14 degrees in the rotated latitude–longitude coordinates. The initial and boundary conditions were specified from the NCEP "Aviation" global data. The 24 hour hydrostatic (upper panel) and nonhydrostatic (lower panel) forecasts of the 850 HPa heights starting from 12 UTC April 20, 2001 are shown in Fig. 2 with a 10 m contour interval. The areas shown in the plots are zoomed around the lows located across the border between South Dakota and Minnesota. Except for vertical interpolation, no smoothing was applied to the model produced fields, which in the area shown, do not interfere with model topography. As can

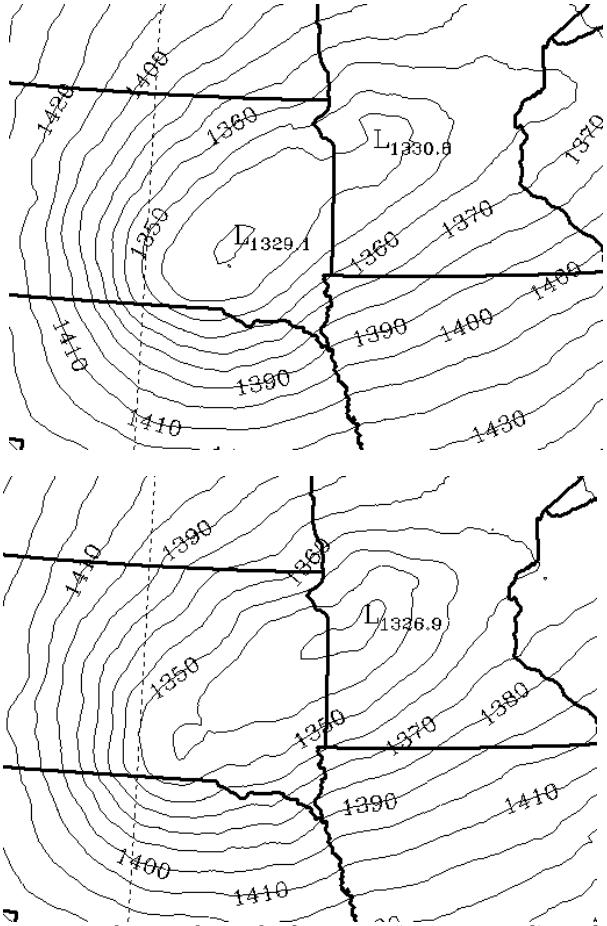

Fig. 2. The 24 hour hydrostatic (upper panel) and nonhydrostatic (lower panel) forecasts of 850 hPa heights from 12 UTC, April 20, 2001. The contour interval is 10 m.

be seen from the figure, considerable differences in details between the two forecasts developed, although their general appearances remained similar. There is a considerable difference in the locations, and considering the scales, the depths of the centers of the lows. However, increased lateral diffusion reduces the differences between the solutions (not shown).

Having in mind the sensitivity of the forecasts to damping, in the next example the lateral diffusion was set to zero, and the damping of the divergent part of flow was set to the minimum necessary to keep the hydrostatic dynamics stable. The 24 hour forecasts of the 850 hPa heights starting from 12 UTC April 20, 2001, are shown in Fig. 3 with a 10 m contour interval. The hydrostatic and nonhydrostatic forecasts are displayed in the upper and the lower panel, respectively.

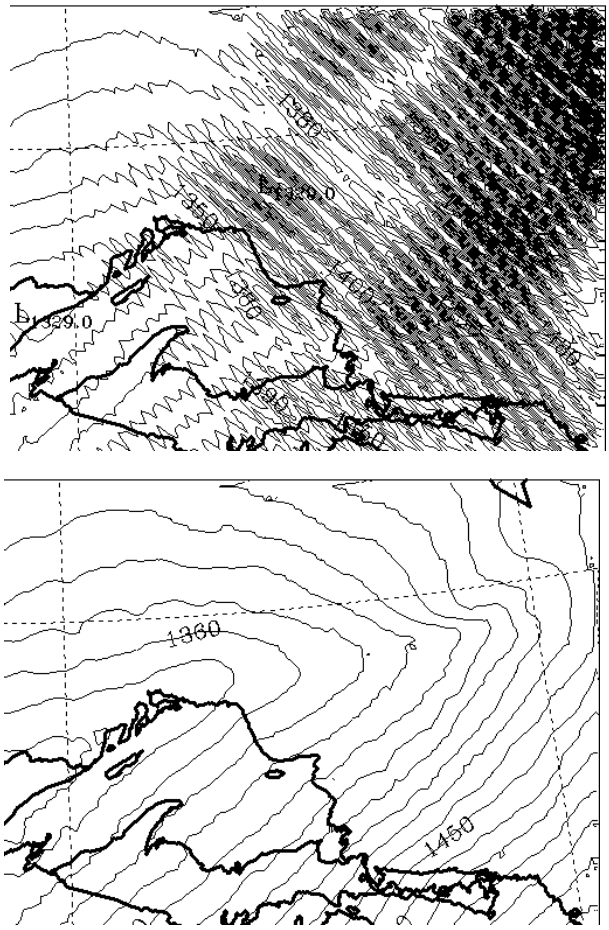

Fig.3. Hydrostatic (upper panel) and nonhydrostatic (lower panel) 24 hour forecasts of 850 hPa heights starting from 12 UTC, April 22, 2001. The contour interval is 10 m.

The areas shown in the plots are zoomed to the North Eastern corner of the integration domain where the noise with considerable amplitude developed in the hydrostatic run. The nonhydrostatic solution does not develop this problem, even with considerably reduced damping. Although the differences between the solutions are not always as large as those shown, it appears that the nonhydrostatic model requires less dissipation than the hydrostatic one in order to control computational instability. This is consistent with the improved computational stability of the nonhydrostatic

model observed in high resolution two-dimensional density current runs by Janjic et al. (2001).

The 24-hour sample forecasts presented here took about 45 minutes to complete on 14 out of 128 four-processor nodes currently available on the NCEP's super computer. The extra cost of the nonhydrostatic module was 13-15% of the execution time. This result indicates that using the domain sizes and resolutions similar to those of the sample forecasts, operational nonhydrostatic forecasting is currently feasible. Moreover, the cost of the nonhydrostatic dynamics was surprisingly modest. A possible problem, however, is that the exchange of data between processors already takes a nontrivial share of the execution time.

For historical reasons, the NCEP Meso model is formulated on the Arakawa grid E. This grid is awkward for coding, and the code is difficult to optimize. For this reason, schemes with the properties analogous to those used in the NCEP E grid model were derived for the B grid, and successfully applied in the SAM nonhydrostatic model developed on a scientific project with the Serbian Academy of Sciences and Arts. The indirect addressing of array elements used on the E grid is unnecessary on the B grid, and the amount of data that has to be exchanged between the processors on massively parallel computers is considerably reduced compared to that on the E grid.

The third example shown here demonstrates a dramatic difference between the hydrostatic and nonhydrostatic solutions encountered with the SAM model. The case considered was the heavy precipitation event that occurred on November 5 1994 in Northern Italy (Buzzi et al. 1998). The SAM forecast was computed using the horizontal resolution of 8 km, and 32 levels in the vertical. The hybrid pressure-sigma vertical coordinate was used, with the sigma coordinate below 400 hPa. The integration domain was 10 degrees by 10 degrees in the rotated latitude–longitude coordinates and had 141 by 141 grid points. The center of the domain was positioned at 7.5^0E and 44^0N.

The 24 hour hydrostatic (upper panel) and nonhydrostatic (lower panel) forecasts of precipitation accumulated over 24 hours are displayed in Fig. 4. The area shown is zoomed over the region where the problem with the hydrostatic dynamics is most pronounced, i.e., the region between Corsica in the South, Italian coastline to the East, and Italian and French mainland in the North. The contours are drawn at 10 mm intervals. Other fields obtained with the hydrostatic dynamics demonstrate similar noisiness (not shown). Switching off the moist processes removes the noise, indicating that the moist processes were responsible for the difficulties in the hydrostatic case. This raises the question of a possible role of moist convection, and whether more active convection would alleviate the problem. Retuning the convection scheme back to the set-up used operationally at NCEP with the horizontal resolution of 22 km, certain improvement was achieved (not shown), but the problem could not be eliminated. Significant increase of lateral diffusion and divergence damping was the only effective method for controlling the problem of the hydrostatic solution.

Fig. 4. Hydrostatic (upper panel) and nonhydrostatic (lower panel) 24 hour forecasts of precipitation accumulated over 24 hours starting from 00 UTC, November 5, 1994. The contour interval is 10 mm.

Note that the 24 hour nonhydrostatic forecast using the described configuration of the SAM model took slightly more than four hours on a 1200 MHz Athlon PC. This result indicates that with the current approach, meaningful nonhydrostatic forecasting is becoming feasible even on PC's and lower end workstations.

4. Conclusions

The examples shown demonstrate that significant differences between hydrostatic and nonhydrostatic forecasts can develop even at relatively coarse horizontal resolution of 8 km. The nonhydrostatic dynamics appears to be computationally more robust in the sense that it requires less computational damping for stability.

The sample forecasts indicate that with the current approach meaningful nonhydrostatic NWP using single digit horizontal resolutions is feasible, not only at major centers, but also at universities and local weather centers and research institutes. Moreover, the relatively low cost of the nonhydrostatic dynamics justifies the application of nonhydrostatic dyamics even at medium resolutions.

References

Adcroft, A., C. Hill and J. Marshall, 1997: Representation of topography by shaved cells in a height coordinate ocean model. *Mon. Wea. Rev.*, **125**, 2293–2315.

Arakawa, A. and V. R. Lamb, 1977: Computational design of the basic dynamical processes of the UCLA general circulation model. *Methods in Computational Physics, 17, Academic Press*, 173-265.

Bryan, K., 1969: A numerical method for the study of the circulation of the World Ocean. *J. Comp. Phys*, **4**, 347-376.

Buzzi, A., N. Tartaglione and P. Malguzzi, 1998: Numerical Simulations of the 1994 Piedmont Flood: Role of Orography and Moist Processes. *Mon. Wea. Rev.*, **126**, 2369–2383.

Chen, F., Z. Janjic and K. Mitchell, 1997: Impact of atmospheric surface–layer parameterization in the new land–surface scheme of the NCEP mesoscale Eta model. *Boundary–Layer Meteorology* **48**, 391–421.

Gallus W. A., Jr., 2000: The Impact of Step Orography on Flow in the Eta Model: Two Contrasting Examples. *Weather and Forecasting*:, **15**, 630–639.

Gallus W. A., Jr. and J. B. Klemp, 2000: Behavior of Flow over Step Orography. *Mon. Wea. Rev.*, **128**, 1153–1164.

Janjic, Z. I., 1977: Pressure gradient force and advection scheme used for forecasting with steep and small scale topography. *Contrib. Atmos. Phys.*, **50**, 186–199.

_____, 1979: Forward–backward scheme modified to prevent two–grid–interval noise and its application in sigma coordinate models. *Contrib. Atmos. Phys.*, **52**, 69–84.

_____, 1984: Non–linear advection schemes and energy cascade on semi–staggered grids. *Mon. Wea. Rev.*, **112**, 1234–1245.

_____, 1990: The step–mountain coordinate: physical package. *Mon.Wea.Rev.*, **118**, 1429–1443.

_____, 1994: The step–mountain eta coordinate model: further developments of the convection, viscous sublayer and turbulence closure schemes. *Mon. Wea. Rev.*, **122**, 927–945.

_____, 1996a: The Mellor–Yamada level 2.5 scheme in the NCEP Eta model. Eleventh Conf. on NWP, Norfolk, VA, 19–23 August 1996; AMS, Boston, MA, 333–334.

_____, 1996b: The surface layer in the NCEP Eta model. Eleventh Conf. on NWP, Norfolk, VA, 19–23 August 1996; AMS, Boston, MA, 354–355.

_____, 1997: Advection scheme for passive substances in the NCEP Eta model. *Research Activities in Atmospheric and Oceanic Modelling*, WMO, Geneva, CAS/JSC WGNE, 3.14.

_____, 2000: Comments on "Development and Evaluation of a Convection Scheme for Use in Climate Models. *J. Atmos. Sci.*, Vol. **57**, p. 3686

_____, 2001: A Nonhydrostatic Model Based on a New Approach. *Meteorol. Atmos. Phys.* Accepted for publication.

Janjic, Z. and A. Wiin–Nielsen, 1977: On geostrophic adjustment and numerical procedures in a rotating fluid. *J. Atmos. Sci.*, **34**, 297–310.

Janjic, Z. I., F. Mesinger and T. L. Black, 1995: The pressure advection term and additive splitting in split-explicit models. *Quart. J. Roy. Meteorol. Soc.*, **121**, 953-957.

Janjic, Z. I., J. P. Gerrity, Jr. and S. Nickovic, 2001: An Alternative Approach to Nonhydrostatic Modeling. *Mon. Wea. Rev.*, **129**, 1164-1178.

Janjic, Z. I., and G. DiMego, 2001: Effects of Mountain Representation and Nonhydrostatic Dynamics in a Case of Orographic Precipitation. Preprints, Symposium on Precipitation Extremes: Prediction, Impacts and Responses. 81st Annual Meeting of the American Meteorological Society, January 14-19, 2001, Albuquerque, NM, AMS, Boston, MA, in print.

Janjic, T. Z., 1998: Comments on "A finite–volume integration method for computing pressure gradient force in general vertical coordinates" by Shian–Jiann Lin (July B, 1997, **123**,1749–1762). *Quart. J. Roy. Meteorol. Soc.*, **124**, 2527–2529.

McDonald, B.E., J.D. Horel, C.J. Stiff and W.J. Steenburgh, 1998: Observations and simulations of three downslope wind events over the northern Wasatch mountains. Preprint 16th Conference on WAF at Phoenix, AMS, Boston, MA, 62-64.

Mesinger, F., Z.I. Janjic, S. Nickovic, D. Gavrilov and D.G. Deaven, 1988: The step–mountain coordinate: model description and performance for cases of Alpine lee cyclogenesis and for a case of an Appalachian redevelopment. *Mon.Wea. Rev.*, **116**, 1493–1518.

Staudenmeier, M., Jr. and J. Mittelstadt, 1998: Results of the Western Region evaluation of the Eta-10 Model. Preprints, Twelfth Conf. on NWP, Phoenix, AZ, 11-16 January, 1998; AMS, Boston, MA, 131-134.

Zhao, Q., and F.H. Carr, 1997: A prognostic cloud scheme for operational NWP models. *Mon. Wea. Rev.*, **125**, 1931–1953.